



Revista Ambiente & Água

ISSN: 1980-993X

Instituto de Pesquisas Ambientais em Bacias Hidrográficas

Ferrari, Ana Maria; Germiniano, Talitha Oliveira; Savoia, Jaqueline Elisabete; Marques, Rubiane Ganascim; Ribeiro, Valquíria Aparecida dos Santos; Ueda, Ana Cláudia
CaTiO₃ Perovskite in the Photocatalysis of Textile Wastewater
Revista Ambiente & Água, vol. 14, no. 3, 2019
Instituto de Pesquisas Ambientais em Bacias Hidrográficas

DOI: 10.4136/ambi-agua.2336

Available in: <http://www.redalyc.org/articulo.oa?id=92860487014>

- How to cite
- Complete issue
- More information about this article
- Journal's homepage in redalyc.org

UAEM redalyc.org

Scientific Information System Redalyc

Network of Scientific Journals from Latin America and the Caribbean, Spain and Portugal







Project academic non-profit, developed under the open access initiative



CaTiO₃ Perovskite in the Photocatalysis of Textile Wastewater

ARTICLES doi:10.4136/ambi-agua.2336

Received: 01 Oct. 2018; Accepted: 31 Mar. 2019

Ana Maria Ferrari^{1*}; Talitha Oliveira Germiniano¹; Jaqueline Elisabete Savoia²;
Rubiane Ganascim Marques¹; Valquíria Aparecida dos Santos Ribeiro³;
Ana Cláudia Ueda¹

¹Universidade Tecnológica Federal do Paraná (UTFPR), Apucarana, PR, Brasil
Programa de Pós-Graduação em Engenharia Ambiental (PPGEA). E-mail: analima@utfpr.edu.br,
talithaxd@hotmail.com, rubiane@utfpr.edu.br, anaueda@utfpr.edu.br

²Universidade Tecnológica Federal do Paraná (UTFPR), Apucarana, PR, Brasil
Coordenação de Engenharia Química. E-mail: savoia.jaqueline@gmail.com

³Universidade Tecnológica Federal do Paraná (UTFPR), Apucarana, PR, Brasil
Coordenação de Engenharia Têxtil. E-mail: valquiria@utfpr.edu.br

*Corresponding author

ABSTRACT

Perovskite-type CaTiO₃ material was synthesized by the polymeric precursor method and characterized. The powder was applied as a promising alternative to TiO₂ photocatalyst. Photocatalytic reaction parameters were optimized by surface analysis methodology on the degradation of methylene blue under UV radiation. After optimization, complex textile- and tannery wastewaters were treated and the COD reduction was evaluated. At optimized conditions (pH=11.2 and 1 g L⁻¹ of catalyst concentration), the results obtained for the photodegradation of the real wastewater after 240 min of irradiation were 45% COD reduction for both effluents. The reactions were adjusted to the pseudo first order kinetic and the rate constants were 2.07 x 10⁻³ (min⁻¹) and 2.23 x 10⁻³ (min⁻¹) for COD reduction for textile- and tannery wastewaters, respectively.

Keywords: calcium titanate, dye, photocatalyst, real wastewater, response surface analysis.

Perovskitas do tipo CaTiO₃ na Fotocatálise de Efluentes Têxteis

RESUMO

O material CaTiO₃ do tipo perovskita foi sintetizado pelo método dos precursores poliméricos e caracterizado. Os parâmetros da reação fotocatalítica foram otimizados pela metodologia de análise de superfície de resposta na degradação do azul de metileno sob radiação UV. Após a otimização, as águas residuais têxteis e de curtume foram tratadas e a redução da DQO foi avaliada. Em condições otimizadas (pH = 11,2 e 1 g L⁻¹ de concentração de catalisador), os resultados obtidos para a fotodegradação dos efluentes reais após 240 min de irradiação foram de 45% de redução de DQO para os dois efluentes. As reações foram ajustadas para a cinética de pseudo primeira ordem e as constantes de velocidade foram 2,07 x 10⁻³ (min⁻¹) e 2,23 x 10⁻³ (min⁻¹) para redução de DQO para o efluente têxtil e de curtume, respectivamente.

Palavras-chave: efluente de curtume, efluente têxtil, fotocatalisador, fotocatalise, perovskita, titanato de cálcio.



This is an Open Access article distributed under the terms of the Creative Commons Attribution License, which permits unrestricted use, distribution, and reproduction in any medium, provided the original work is properly cited.

1. INTRODUCTION

It is well known that industries strongly contribute to the contamination of water bodies, particularly the textile and leather industries, since they use a large volume of water in their processes, generating large amounts of effluents. The wastewater from these industries present high organic loads, marked color and resistance to biodegradation, among other aggravating factors (Schmidt *et al.*, 2013). The dyeing of animal skin products as well as mechanical and hydrothermal resistance by the tannery industries is one of the most pollutant processes in terms of the complexity of the effluent generated, which has high organic and inorganic loads, strong color, solids, and specific pollutants such as chromium (Hasegawa *et al.*, 2014; Sauer *et al.*, 2006). Despite the conventional physical-chemical and biological treatments, most of effluents released to aquatic ecosystems present high concentrations of organic matter, toxic metals, color and total solids.

As a result, industrial wastewater has received a great deal of attention regarding its treatment. New methods are suggested, and a variety of research is conducted to offer treatment alternatives that are increasingly efficient, reduce or do not generate waste, and are economically viable. Among the alternative methods, the Advanced Oxidative Processes (AOPs) have stood out as a versatile, rapid and highly efficient pollutant degradation method. Among the AOP approaches, heterogeneous photocatalysis is one of the most promising and high potential methods for wastewater treatment (Ba-Abbad *et al.*, 2017; Lee and Hamid, 2005). The process is based on the irradiation of a semiconductor oxide, with photons whose energy is equal to or greater than the band gap energy of the semiconductor, generating holes in the valence band as electrons are promoted to the conduction band, leading to the formation of active sites capable of promoting redox reactions.

Perovskite-type oxides with ABO_3 structural formula have the orthorhombic structure in their natural form (Hu *et al.*, 1992). Calcium titanate ($CaTiO_3$) is a well-known and one of the most important perovskites and has recently attracted a lot of interest, since it covers a wide range of applications (Lozano-Sánchez *et al.*, 2015; Ye *et al.*, 2014) due to its structural characteristics: high chemical stability, low cost and ease of synthesis (Zhuang *et al.*, 2014).

Several studies have reported the degradation of pollutants using $CaTiO_3$. Huo *et al.* (2014) evaluated the photocatalytic activity of $CaTiO_3$ for the degradation of methyl orange dye and obtained a 96% removal percentage after 3 hours of UV irradiation. Zhuang *et al.* (2014) reported the photo-oxidation of Arsenic (III) to Arsenic (V) using $CaTiO_3$ and achieved excellent photocatalytic activity for As (III) removal (up to 98.4%) in aqueous solution under UV-254 nm irradiation. Otsuka-Yao-Matsuo *et al.* (2003) studied the degradation of methylene blue with the addition of calcium titanate to TiO_2 and observed an increase in photocatalytic activity. Han *et al.* (2016) evaluated the degradation of methylene blue using $CaTiO_3$ synthesized by the hydrothermal method as photocatalyst. Additionally, it has been reported that $CaTiO_3$ can exhibit superior photocatalytic performance on the removal of other organic and inorganic pollutants and formation of hydrogen and oxygen from the photolysis of water (Liu *et al.*, 2014; Mizoguchi *et al.*, 2002).

Real wastewaters are complex and contain a wide range of compounds. An overall mechanism for photodegradation of real textile industrial wastewater is proposed as follows: (I) the semiconductor must be activated by proper radiation source; (II) electron-hole pairs are generated on the surface; (III) oxidizing species such as OH^\bullet are formed on the surface; (IV) highly reactive hydroxyl radicals oxidize the dye molecules as follows: $Dye + OH^\bullet \rightarrow$ degradation and (V) the UV irradiation is concomitantly used in a photo sensitization process, in which the sensitizer (the dye) absorbs radiation to yield an excited state of the sensitizer. The dye radicals inject electrons to the conduction band of the catalyst and convert to dye^{+} . The formed dye^{+} radical ions react with dye molecules in the same way of the reaction of hydroxyl

radicals, promoting mineralization (Khan *et al.*, 2016; Akpan and Hameed, 2009).

Only a very few papers report the treatment of real effluents, such as textile and tannery wastewater. Highlighting our recent work (Ferrari-Lima *et al.*, 2017), evaluated the photodegradation of methylene blue and the combined treatment of a real textile wastewater by coagulation/flocculation/photocatalysis using the mesoporous perovskites CaTiO₃ and CaTi_xZr_(1-x)O₃ ($x = 0.0.25.0.50.0.75$ and 1.0) prepared by the polymeric precursor method. The best results were achieved with CaTiO₃.

With this background, CaTiO₃ synthesized by the polymeric precursor method was applied to the photodegradation of textile and tannery wastewater, and COD reduction was adjusted to the pseudo-first order kinetics. Toxicity evaluation was performed with *Lactuca sativa* seeds. The reaction parameters have also been optimized by means of response surface analysis methodology on the photocatalysis of methylene blue.

2. METHODS

2.1. Catalyst preparation and characterization

CaTiO₃ powders were prepared by the polymeric precursor method, according to the previously published methodology (Ferrari-Lima *et al.*, 2017). Calcium acetate [Ca(C₂H₃O₂)₂] (97% Aldrich), titanium butoxide (C₁₆H₃₆O₄Ti) (97% Aldrich), ethylene glycol (C₂H₆O₂) (99.5% Synth) and citric acid (C₆H₈O₇) (99.5%, Dinâmica) were used as raw materials. In the experimental procedure, Ti citrate was formed by the dissolution of C₁₆H₃₆O₄Ti in citric acid aqueous solution at 75°C under constant stirring. This citrate solution was then stirred and heated at 90°C, and then Ca(C₂H₃O₂)₂ was dissolved in stoichiometric quantity into the Ti citrate solution. After solution homogenization, C₂H₆O₂ was added in order to promote the citrate polymerization. The citric acid/ethylene glycol mass ratio was fixed at 60:40 (wt%). The resulting solution was heated at 90°C under constant stirring to eliminate water and form a polymeric resin, which was then placed in a conventional furnace and annealed at 350°C for 4 h. Finally, the obtained precursors were heat treated at 700°C for 2 h. XRD analysis was performed in a Rigaku diffractometer Model MiniFlex 600, with CuK α ($\lambda = 1.5406 \text{ \AA}$) in a 2θ range of 3°–120°, at a nominal power source of 40 kV \times 15 mA. Textural analysis was performed by nitrogen adsorption–desorption isotherms at 77 K using Quantachrome NOVA 1200 equipment. Photoacoustic spectroscopy (PAS) analysis was carried out in a self-designed apparatus and scanning electron microscopy analysis was performed on a JEOL JSM-6010 Scanning Electron Microscope equipped with an EDS System. Finally, the zero point of charge (pH_{ZPC}) was determined according to the methodology proposed by Keng and Uehara (1974).

2.2. Photocatalytic degradation studies

The photoactivity of the prepared powder was measured in the photodegradation of methylene blue (MB) 10 mg L⁻¹ aqueous solution, a textile and a tannery wastewater collected after conventional biologic treatment system. Photocatalytic tests were performed under ultraviolet (UV) irradiation in a slurry bath reactor. In a typical experiment, the CaTiO₃ photocatalyst was suspended in 25 mL of the solution and allowed to stir for 30 min in the dark to attain adsorption equilibrium before irradiation. First, preliminary experiments were carried out in order to outline the Central Composite Design (CCD) for application on the MB photodegradation optimization. After optimization, the best values found for pH and catalyst loading were applied to the photodegradation of two types of real wastewater. All the experiments have been performed in duplicate.

2.3. Response surface methodology

The response surface methodology (RSM) has been successfully applied for the optimization of photocatalytic systems, for example by Soltani *et al.* (2014). In this study, RSM

was used to optimize the two parameters, CaTiO₃ loading and initial pH for the degradation of MB. Since the negative influence of the pollutant concentration on the photocatalytic reaction is well known, only CaTiO₃ loading and initial pH were selected as independent variables, while the degradation percentage of MB was the output response variable. Other factors, such as stirring rate, temperature and light intensity were held constant. The photocatalytic tests were carried out over a multi-position magnetic stirrer, irradiated with a 60W UV-C lamp array. Table 1 shows the ranges and levels of independent variables.

Table 1. Independent variables and experimental range for degradation of MB under UV-C radiation.

Factor	Symbol	Range				
		-α	-1	0	+1	+α
pH	x ₁	2.8	4.0	7.0	10.0	11.2
CaTiO ₃ loading (mg L ⁻¹)	x ₂	0.3	0.5	1.0	1.5	1.7

Central composite design (CCD) was chosen to investigate the combined effect of the two independent variables by 11 sets of experiments, including three replications at the center points.

By using RSM, the results were matched to an empirical quadratic polynomial as follows (Equation 1) (Montgomery, 2008):

$$Y = \beta_0 + \sum_{j=1}^k \beta_j X_j + \sum_{j=1}^k \beta_{jj} X_j^2 + \sum_i \sum_{<j=2}^k \beta_{ij} X_i X_j + e_i \quad (1)$$

Where Y is the response, X_i and X_j are the variables, β is the regression coefficient, k is the number of factors studied and optimized in the experiment, and e_i is the random error.

2.3.1. Model fitting and statistical analysis

For the graphical analyses, ANOVA (Analysis of variance) has been used in order to define the interaction between the process variables and the responses for statistical parameters assessment. The statistical significance was checked by F-test and the accuracy of the fitted polynomial model was determined by the coefficient of R². The significant model terms were evaluated by the probability value (P-value) at 95% confidence interval. A number of statistical analyses such as the normal plot, residual analysis, main and interaction effects and contour plot was examined.

2.4. Textile and tannery wastewater photodegradation

After optimization of MB decomposition, the optimized conditions were applied to the photodegradation of two types of real wastewater: from a textile- and a tannery industry, presenting chemical oxygen demands of 148 mg L⁻¹ and 323 mg L⁻¹, respectively.

Therefore, the photocatalytic tests were carried out in a 500 mL self-designed Inox Reactor (Figure 1). The temperature of the reaction was maintained around 25.0 ± 0.5°C by using a cooling jacket. A 125-W mercury lamp without a bulb was used as a UV source and inserted into the reactor chamber protected by a quartz tube. An aquarium air pump was used as an oxygen source. Aliquots were collected periodically and analyzed by chemical oxygen demand (COD).

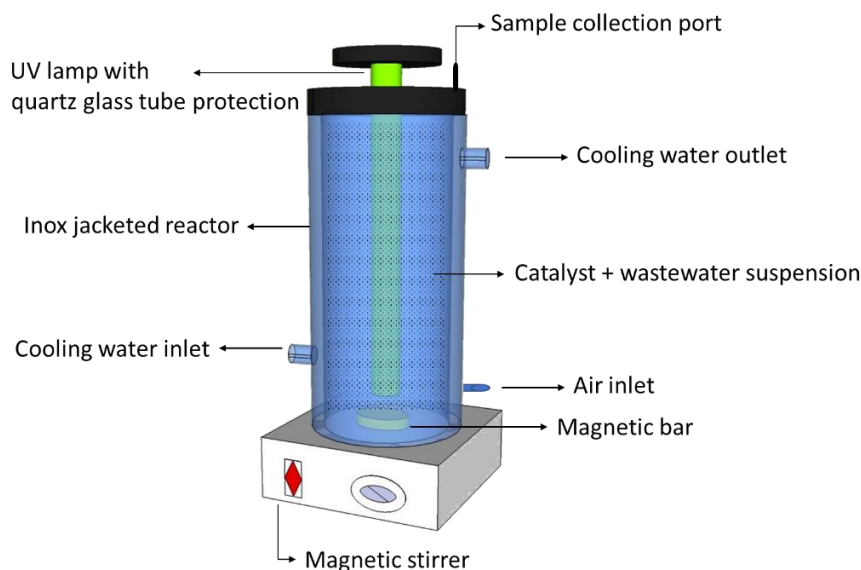


Figure 1. Schematic diagram of the photoreactor.

2.5. Phytotoxicity of real wastewater to *Lactuca sativa* seeds

Sensitive, short-term and simple ecotoxicological bioassays have been performed with *Lactuca sativa* seeds. For the phytotoxicity tests, Petri dishes were lined with a filter paper where the sample unit containing 20 lettuce seeds (*Lactuca sativa*) with 80.0% of germination index was deposited, being moistened with 7.0 mL of distilled water for the negative, NaCl (1 mol L⁻¹) for the positive control and with the samples to be tested (textile- and tannery effluents with and without photocatalytic treatment). The plates were closed and kept at room temperature for 120 h. The assay was conducted in triplicate. The percentage of relative germination (% GR) was calculated by means of Equation 2, in which SSG is the number of seeds germinated in the sample and number CSG represents the number of seeds germinated in the negative control. According to Priac *et al.* (2017), these bioassays are simple, inexpensive and only require a relatively small amount of sample. Lettuce is one of the most-common plant species recommended by the US Environmental Protection Agency and the US Food and Drug Administration for this kind of bioassay (USEPA, 1996; FDA, 1987).

$$\%RG = \frac{n^{SSG}}{n^{CSG}} \times 100 \quad (2)$$

3. RESULTS AND DISCUSSION

3.1. Characteristics of CaTiO₃

The main characteristics of the photocatalyst are presented in Table 2. The synthesized powder showed mesoporous structure with an average pore diameter of 44.8 Å and orthorhombic phase. Specific surface area and band gap energy are in good agreement with literature (Mohammadi and Fray, 2013; Lozano-Sánchez *et al.*, 2015).

Table 2. Characteristics of CaTiO₃.

Parameter	Value
Crystallite size (Å)	269
BET specific surface area (m ² g ⁻¹)	34.6
Average pore diameter (Å)	44.8
pH _{ZPC}	10.1
Band-gap energy (eV)	3.44

Figure 1 presents the XRD and UV-Vis absorption spectra of CaTiO_3 . The orthorhombic phase belonging to the space group Pbnm was identified by ICDD (number 01-081-0562). It can be noted that the catalyst mainly absorbs in the ultraviolet region. As shown in Figure 2, the EDS spectra of CaTiO_3 revealed the existence of well-distributed Ti, O and Ca in the sample. However, the material presented a non-uniform morphology. The elemental composition indicates that the presence of impurities besides carbon was not detected and the Ca/Ti ratio is 1.17:1.

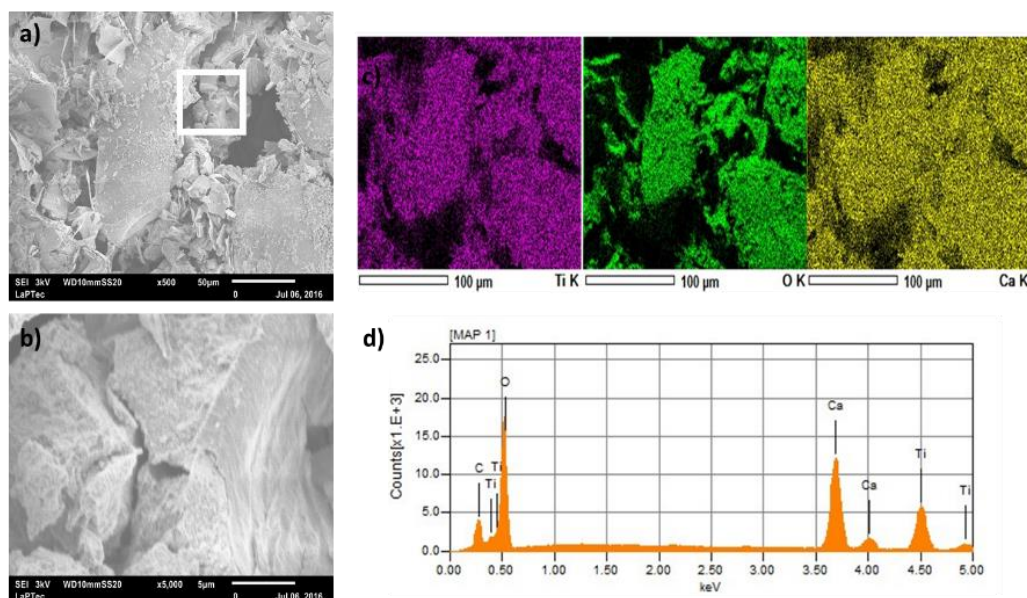


Figure 2. SEM images of CaTiO_3 fabricated by the polymeric precursor method: x500 (a), x5000 (b), elemental mapping (c) and (d).

3.2. Photocatalytic bleaching of methylene blue

Aiming to optimize the reaction conditions of MB degradation, a CCD with a total number of 11 experiments was applied for the response surface modelling. The software suggested quadratic model. Interactions among the two independent variables were considered in each run to investigate the validity of the photocatalytic treatment. The removal efficiencies ranged from 22% to 69% for MB. By using RSM, the results were matched to an empirical quadratic polynomial model and were written in terms of coded factors as shown in Equation 3.

$$Y = 23.01 + 34.09x_1^2 + 22.93x_2^2 \quad (3)$$

For MB removal, the quadratic terms x_1^2 and x_2^2 are significant, as the p-value for them is <0.05 . From the values of the coefficients in the regression model, the order in which the independent variables affect the degradation of MB is, $\text{pH} (x_1) > \text{catalyst loading} (x_2)$, and the effect is positive for both.

The correlation coefficient R^2 for the polynomial represented by Equation 3 had a value of 0.83, indicating a good correlation of the experimental data with the proposed model in the range studied. Values above 0.80 are acceptable for surface response modeling (Suárez-Escobar *et al.*, 2016). Additionally, the predicted R^2 (0.83) is close to the adjusted R^2 (0.89), which implies good predictability of the model (Lee and Hamid, 2015).

The optimum values for the independent variables were found using three-dimensional response surface analysis of the independent and dependent variables. The effect of the independent variables on the decolorization of MB is shown on Figure 3.

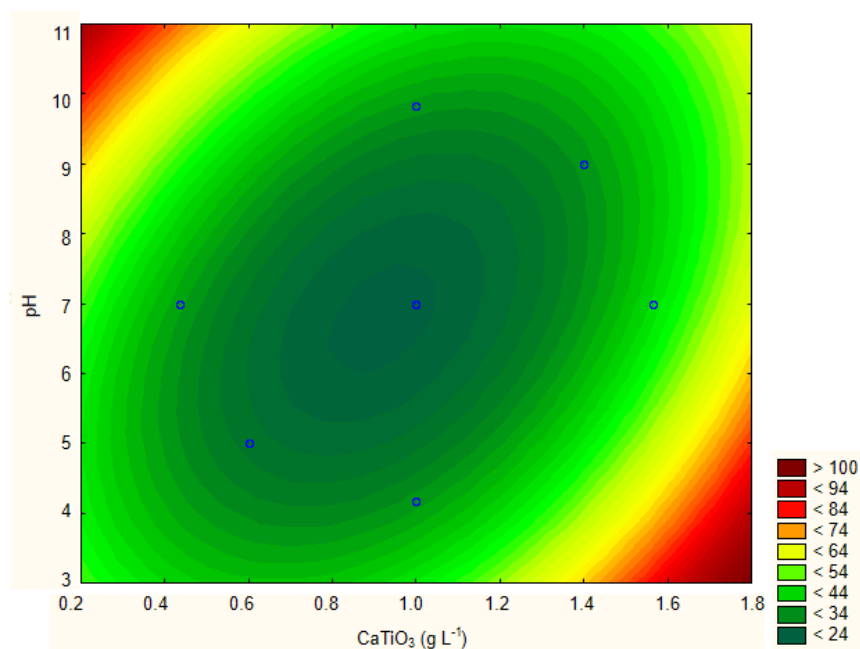


Figure 3. Contour plot of MB removal for the photocatalytic process after 180 min of UV irradiation with CaTiO₃.

Figure 3 depicts the influence of the CaTiO₃ dosage and pH on the degradation of MB. As illustrated in the plots and by Equation 3, the degradation percentage increases with increasing catalyst loading. The increase in catalyst loading enhances the number of active sites on the catalyst surface, increasing the number of hydroxyl radicals responsible for the degradation MB molecules. Degradation is also increased by increasing pH. This may be because of the higher color intensity of MB in the acidic pH range. Additionally, the p_H_{ZPC} of CaTiO₃ is around 10, and at pH smaller than p_H_{ZPC}, the surface of the catalyst is positively charged; hence, at low pH the dye forms multilayers on the catalyst particles, preventing the UV light from reaching their surface (Yang *et al.*, 2014).

3.3. Kinetic study of textile and tannery wastewater photodegradation

After 180 min of irradiation, a maximum removal for MB of 69% with a catalyst loading of 1.0 g L⁻¹ and pH of 11.2 was obtained. In order to investigate the behavior of these conditions in a real situation, the kinetic study was performed for the real textile and tannery wastewater. The results are shown in Figure 4.

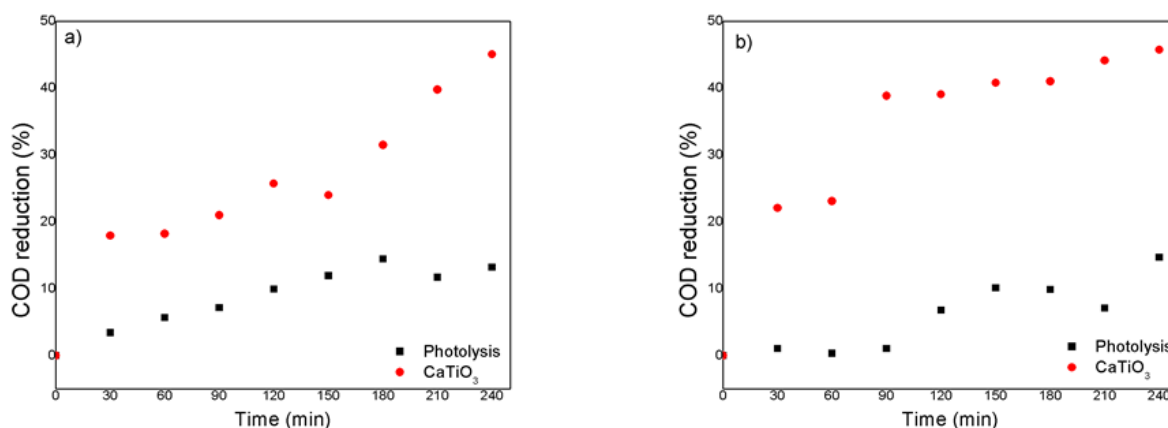


Figure 4. Kinetic behavior of the COD removal for (a) textile and (b) tannery wastewater after photocatalysis with CaTiO₃. Catalyst loading=1.0 g L⁻¹, pH=11.2.

A photolysis study was carried out and after a reaction time of 240 minutes about 10% of the wastewater was degraded. After that, the textile and the tannery effluents were treated by photocatalysis with CaTiO_3 during the same time interval. Since CaTiO_3 synthesized in this work has shown to be better than TiO_2 P25 in our previous study (Ferrari-Lima *et al.*, 2017), no comparison was made with this standard catalyst.

Kinetic data for COD removal were adjusted to the pseudo-first order model, obtaining an apparent kinetic constant “k” of $2.07 \times 10^{-3} \text{ min}^{-1}$ ($R^2 = 0.9084$) for the textile wastewater, and an apparent kinetic constant of $2.23 \times 10^{-3} \text{ min}^{-1}$ ($R^2 = 0.8199$) for the tannery wastewater. A maximum removal of 45% and 46% of COD was achieved for textile and tannery wastewater, respectively, after 240 min of irradiation. Yang *et al.* (2014) reported a pseudo-first order kinetic constant of $3.1 \times 10^{-3} \text{ min}^{-1}$ for the degradation of MB with pure CaTiO_3 under UV-visible light, and Han *et al.* (2016) reported a pseudo-first order kinetic constant of $1.80 \times 10^{-3} \text{ min}^{-1}$ for the degradation of methylene blue with the same catalyst with a Xe lamp. In our previous work (Ferrari-Lima *et al.*, 2017), a kinetic constant of $7.3 \times 10^{-3} \text{ min}^{-1}$ was found for the photodegradation of a coagulation/flocculation pre-treated textile wastewater with CaTiO_3 under UV-light at the same reactor discussed in this section. Other reports regarding the treatment of a real wastewater by photocatalysis with CaTiO_3 are rare.

3.4. Phytotoxicity assessment

One drawback of treating wastewater by advanced oxidation processes is the possible generation of toxic by-products. In this sense, a toxicity evaluation of the wastewater before and after treatment is mandatory. In this work, a simple phytotoxicity test was performed with the textile- and tannery wastewaters. The toxicity comparison between the effluents before and after the photocatalytic treatment was evaluated according to the percentage of germination (% RG), calculated according to Equation 2. Figure 5 shows the results.

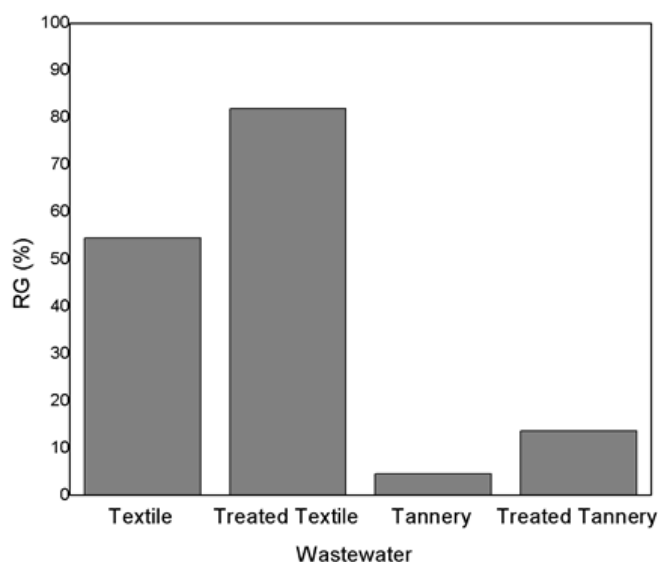


Figure 5. Percentage of relative germination of textile- and tannery wastewater before and after photocatalysis with CaTiO_3 .

Textile wastewater, polished by photocatalysis (240 min of irradiation), showed an increase of about 27% (from 55% to 82%) in the relative germination index when compared to the wastewater without treatment. Garcia *et al.* (2009) reached 75% of germination after photocatalysis of textile wastewater with TiO_2 P25 with the same irradiation time. The treated tannery wastewater also showed an increase in RG index (9%) compared to the wastewater

conventionally treated by the industry. Considering that values of ICCR below 80% indicate a root-growth inhibition effect (Young *et al.*, 2012), the germination difference between the studied effluents is remarkable. In the tannery wastewater, the germination index was much lower than that observed for the textile wastewater even after the photocatalytic treatment. This may be due to the possible high concentration of toxic pollutants such as chromium VI, which is often used in tannery industries. High concentrations of organic matter could also explain its toxicity, as well as other concentrated components, such as salts (Elabbas *et al.*, 2016).

Hasegawa *et al.* (2014) treated tannery wastewater by photocatalysis, applying ZnO, and reached over 97% of COD while decreasing toxicity to *Artemia salina* nauplii after 240 min. However, no reference relating to a *Lactuca sativa* germination index analysis of photocatalysis-treated tannery wastewater has been found as of this writing.

4. CONCLUSION

Perovskite-type CaTiO₃, with mesoporous structure were synthesized and the photocatalytic degradation of methylene blue were optimized by means of response surface methodology. Degradation of 69% was achieved after 180 min of irradiation. Optimized conditions have been applied to the photodegradation of textile- and tannery wastewater after conventional treatment, and an apparent kinetic constant of about 0.002 min⁻¹ was obtained for both effluents. After photocatalysis, a reduction of about 45% of COD was achieved for both textile- and tannery wastewater, and the phytotoxicity of the effluents to *Lactuca sativa* seeds was reduced.

5. ACKNOWLEDGMENTS

The authors would like to thank the Brazilian agency CNPq (459057/2014-6) for financial support.

6. REFERENCES

- AKPAN, U. G.; HAMEED, B. H. Parameters affecting the photocatalytic degradation of dyes using TiO₂ based photocatalysts: A review. **Journal of Hazardous Materials**, v. 170, p. 520-529, 2009.
- BA-ABBAD, M. M.; TAKRIFF, M. S.; SAID, M. *et al.* **International Journal of Environmental Research**, v. 11, p. 461, 2017. <https://dx.doi.org/10.1007/s41742-017-0041-3>
- ELABBAS, S.; MANDI, L.; BERREKHIS, F.; PONS, M. N.; LECLERC, J. P.; OUAZZANI, N. Removal of Cr (III) from chrome tanning wastewater by adsorption using two natural carbonaceous materials: Eggshell and powdered marble. **Journal of Environmental Management**, v. 166, p. 589-595, 2016.
- FERRARI-LIMA, A. M.; UEDA A. C.; BERGAMO E. A.; MARQUES R. G. *et al.* Perovskite-type titanate zirconate as photocatalyst for textile wastewater treatment. **Environmental Science and Pollution Research**, v.24, p.12529–12537, 2017. <https://doi.org/10.1007/S11356-016-7590-4>
- GARCIA, J.C.; SIMIONATO, J.I.; ALMEIDA, V.D.C.; PALÁCIO, S.M.; ROSSI, F.L.; SCHNEIDER, M.V.; SOUZA, N.E.D. Evolutive follow-up of the photocatalytic degradation of real textile effluents in TiO₂ and TiO₂/H₂O₂ systems and their toxic effects on *Lactuca sativa* seedlings. **Journal of the Brazilian Chemical Society**, v. 20, p.1589–1597, 2009.

- HAN, C.; LIU, J.; YANG, W.; WU, Q.; YANG, H.; XUE X. Enhancement of photocatalytic activity of CaTiO_3 through HNO_3 acidification. **Journal of Photochemistry and Photobiology A: Chemistry**, v.322-323, p.1-9, 2016. <https://doi.org/10.1016/J.jphotochem.2016.02.012>
- HASEGAWA, M. C.; DANIEL, J. F. S.; TAKASHIMA K.; BATISTA, G. A.; SILVA, S. M. C. P. COD removal and toxicity decrease from tannery wastewater by zinc oxide-assisted photocatalysis: a case study. **Environmental Technology**, v.35, p.1-6, 2014.
- HU, M.; WENK, H-R.; SINITSYNA D. Microstructures in natural perovskites. **American Mineralogist**, v.77, p.359-373, 1992.
- HUO, Y. S.; YANG, H.; XIAN, T.; JIANG, J. L.; WEI, J. Q.; LI, R. S.; FENG, W. J. A polyacrylamide gel route to different-size CaTiO_3 nanoparticles and their photocatalytic activity for dye degradation. **Journal of Sol-Gel Science and Technology**, v. 71, p. 254-259, 2014.
- KENG, J. C. W.; UEHARA, G. **Proceedings, Soil Crop Science Society of Florida**, v. 33, p. 119-126, 1974.
- KHAN, W. Z.; NAJEEB, I; ISHTIAQUE, S. Photocatalytic Degradation of a Real Textile Wastewater using Titanium Dioxide, Zinc Oxide and Hydrogen Peroxide. **The International Journal Of Engineering And Science**, v. 5, n. 7, p. 61-70, 2016.
- LEE, K. M.; HAMID, S. B. A. Simple Response Surface Methodology: Investigation on Advance Photocatalytic Oxidation of 4-Chlorophenoxyacetic Acid Using UV-Active ZnO Photocatalyst. **Materials**, v. 8, p. 339-354, 2015. <https://dx.doi.org/10.3390/ma8010339>
- LIU, S.; QU, Y.; LI, R.; WANG, G.; LI, Y. Photocatalytic activity of MTiO_3 ($\text{M} = \text{Ca}, \text{Ni}, \text{and Zn}$) nanocrystals for water decomposition to hydrogen. **Journal of Materials Research**, v. 29, p. 1295-1301, 2014. <https://dx.doi.org/10.1557/jmr.2014.110>
- LOZANO-SÁNCHEZ, L. M.; OBREGÓN, S.; DÍAZ-TORRES, L. A.; LEE, S.W.; RODRÍGUEZ-GONZÁLEZ, V. Visible and near-infrared light-driven photocatalytic activity of erbium-doped CaTiO_3 system. **Journal of Molecular Catalysis A: Chemical**, v. 410, p. 19-25, 2015. <https://doi.org/10.1016/j.molcata.2015.09.005>
- MIZOGUCHI, H.; UEDA, K.; ORITA, M.; MOON, S. C.; KAJIHARA, K.; HIRANO, M.; HOSONO, H. Decomposition of water by a CaTiO_3 photocatalyst under UV light irradiation. **Materials Research Bulletin**, v. 37, p. 2401-2406, 2002. [https://doi.org/10.1016/S0025-5408\(02\)00974-1](https://doi.org/10.1016/S0025-5408(02)00974-1)
- MOHAMMADI, M. R.; FRAY, D. J. Synthesis of highly pure nanocrystalline and mesoporous CaTiO_3 by a particulate sol-gel route at the low temperature. **Journal of Sol-Gel Science and Technology**, v. 68, p. 324–333, 2013. <https://dx.doi.org/10.1007/s10971-013-3173-8>
- MONTGOMERY, D.C. **Design and Analysis of Experiments**. New York: John Wiley & Sons, 2008.
- OTSUKA-YAO-MATSUO, S.; OMATA, T.; UENO, S.; KITA, M. Photobleaching of Methylene Blue Aqueous Solution Sensitized by Composite Powders of Titanium Oxide with SrTiO_3 , BaTiO_3 and CaTiO_3 . **Materials Transactions**, v.44, p.2124-2129, 2003. <https://doi.org/10.2320/matertrans.44.2124>

- PRIAC, A.; BADOT, P.-M.; CRINI, G. Treated wastewater phytotoxicity assessment using *Lactuca sativa*: Focus on germination and root elongation test parameters. **Comptes Rendus Biologies**, v. 340, n. 3, p. 188-194, 2017. <https://doi.org/10.1016/j.crvi.2017.01.002>
- SAUER, T. P.; CASARIL, L.; OBERZINER, A. L. B.; JOSÉ, H. J.; MOREIRA, F. P. M. Advanced oxidation processes applied to tannery wastewater containing Direct Black 38—Elimination and degradation kinetics. **Journal of Hazardous Materials**, v. 135, p. 274–279, 2006. <https://doi.org/10.1016/j.jhazmat.2005.11.063>
- SCHIMIDT, T. M. P.; SOARES, F.R.; SLUSARSKI-SANTANA, V.; BRITES-NÓBREGA, F. F.; FERNANDES-MACHADO, N. R.C. Photocatalytic degradation of textile effluent using ZnO/NaX and ZnO/AC under solar radiation. **Green Design, Materials and Manufacturing Processes**, p. 563-566, 2013. <http://dx.doi.org/10.1201/b15002-109>
- SOLTANI, R. D. C.; REZAEI, A.; KHATAEE, A. R.; SAFARI, M. Photocatalytic process by immobilized carbon black/ZnO nanocomposite for dye removal from aqueous medium: Optimization by response surface methodology. **Journal of Industrial and Engineering Chemistry**, v. 20, n. 4, p. 1861-1868, 2014. <https://doi.org/10.1016/j.jiec.2013.09.003>
- SUÁREZ-ESCOBAR, A.; PATAQUIVA-MATEUS, A.; LÓPEZ-VASQUEZ, A. Electrocoagulation—photocatalytic process for the treatment of lithographic wastewater. Optimization using response surface methodology (RSM) and kinetic study. **Catalysis Today**, v. 266, p. 120–125, 2016. <https://doi.org/10.1016/j.cattod.2015.09.016>
- UNITED STATES. Environmental Protection Agency - USEPA. **Ecological effects test guidelines (OPPTS 850.4200)**: Seed germination, root elongation toxicity test. Washington DC, 1996.
- UNITED STATES. Food & Drug Administration - F.D.A. **Seed germination and root elongation, Environmental Assessment Technical Assistance**. Washington DC, 1987.
- YANG, H.; HAN, C.; XUE, X. Photocatalytic activity of Fe-doped CaTiO₃ under UV-visible light. **Journal of Environmental Science**, v. 26, p. 1489-1495, 2014. <https://doi.org/10.1016/j.jes.2014.05.015>
- YE, M.; WANG, M.; ZHENG, D.; ZHANG, N.; LIN, C.; LIN, Z. Garden-like perovskite superstructures with enhanced photocatalytic activity. **Nanoscale**, v. 6, p. 3576-3584, 2014. <https://dx.doi.org/10.1039/C3NR05564G>
- YOUNG, B. J.; RIERA, N. I.; BEILY, M. E.; BRES P. A.; CRESPO, D. C.; RONCO, A. E. Toxicity of the effluent from anaerobic bioreactor treating cereal residues on *Lactuca sativa*. **Ecotoxicology and Environmental Safety**, v. 76, p. 182-186, 2012. <https://doi.org/10.1016/j.ecoenv.2011.09.019>
- ZHUANG, J.; TIAN, Q.; LIN, S.; YANG, W.; CHEN, L.; LIU, P. Precursor morphology-controlled formation of perovskites CaTiO₃ and their photo-activity for As (III) removal. **Applied Catalysis B: Environmental**, v. 156, p. 108-115, 2014. <https://doi.org/10.1016/j.apcatb.2014.02.015>